



ELSEVIER

Nuclear Physics A 683 (2001) 425–442



www.elsevier.nl/locate/npe

3P_0 study of meson decays in a chiral quark model

R. Bonnaz^a, L.A. Blanco^{b,*}, B. Silvestre-Brac^a, F. Fernández^b,
A. Valcarce^b

^a *Institut des Sciences Nucléaires, 53 Av. des Martyrs, F-38026 Grenoble cedex, France*

^b *Grupo de Física Nuclear, Universidad de Salamanca, E-37008 Salamanca, Spain*

Received 30 March 2000; revised 29 June 2000; accepted 20 September 2000

Abstract

The strong decays of a meson into two mesons are studied in the framework of the 3P_0 model. The meson wave functions are determined by means of a realistic chiral quark model constructed in the baryon sector and comparison is made with a traditional potential of “Coulomb + linear” type. Two different forms for the creation vertex are analyzed. A momentum dependent vertex is proved to be definitively superior. The chiral quark model provides an overall good description of all known transitions and gives results of roughly the same quality as those obtained from phenomenological quark–antiquark potentials. © 2001 Elsevier Science B.V. All rights reserved.

PACS: 12.39.Jh; 14.40.-n; 13.25.-k

Keywords: Nonrelativistic quark model; Meson hadronic decays

1. Introduction

A challenging problem of intermediate energy physics is to explore the consequences of the quark structure in hadron phenomenology because we may gain insight about the nonperturbative QCD regime. To this respect baryon and meson spectra, as well as the hadron–hadron interaction, seem to be the most promising systems. They have been successfully studied within the nonrelativistic quark model relying on simple potentials inspired by QCD, but always independently.

It is surprising that the success of the quark model did not favor a trial to a simultaneous description of the systems mentioned above (baryons and mesons) based on a fundamental quark–quark interaction. There should be a closed connection between meson and baryon dynamics. Confinement should be very similar in both cases, since color forces at large distances are only sensitive to the net color charge of the interacting sources. Thus, whether

* Corresponding author.

E-mail address: luis@mozart.usal.es (L.A. Blanco).

a quark is bound to an antiquark (meson) or to a diquark (baryon) in a color singlet should make no difference at large separation. For similar reasons, the one-gluon exchange force in mesons and baryons are closely related; for identical spins and separations they have in baryons half of the strength than in mesons. Finally, if chiral symmetry is advocated as a mechanism that generates interaction between the constituents of the hadrons, once again it should not make any significant difference to work with mesons or baryons. Obviously, the difference between the two sectors will come from those mechanisms that only act in one of them, as for example annihilation for the meson sector or three-body forces for the baryon sector.

There have been plenty of quark models in the literature, but among them the chiral quark cluster model (χ QM) of Ref. [1] is the only one that has pursued a simultaneous description of the low-energy QCD problems. Applied originally to the nucleon–nucleon (NN) interaction, it has demonstrated the capability to describe the baryon spectra, and recently it provided a quantitative description of the gross features of the meson spectra. Obviously, it is a stringent test for the model, if one takes into account that there are no more than a few parameters, that, in this paper, are taken from the baryon–baryon interaction.

However, the calculation of the spectrum is an average of the wave function of the different mesons and to judge the quality of the model one has to rely on more sensitive observables. Among them, one could choose electromagnetic properties or strong decays. In the first case the transition operator is precisely known, but gauge invariance imposes severe conditions that can hardly be achieved in a nonrelativistic treatment. In the case of strong decays, the transition operator is not known from theoretical principles, although we know the basic Lagrangian of the strong interaction. This is, of course, because we cannot treat always QCD perturbatively. Even for the simple case of the decay of a meson into two mesons or a baryon into a meson and a baryon, different models have been proposed to explain the decay. The elementary emission model, the 3P_0 , the 3S_1 are some examples of the prescriptions used to calculate these processes.

It would be very interesting to connect the different models to more basic QCD properties. A comparative study of hadronic decays using the 3S_1 and 3P_0 models has been performed by Geiger and Swanson [2]; they showed that the 3P_0 structure is largely favored to explain the experimental situation (even if the final state interaction is included). In the same spirit, the work by Ackleh et al. [3] deals with the connection between 3P_0 and scalar confining terms and one-gluon exchange terms resulting from QCD. Here again, the 3P_0 structure is compatible with what can be expected on more fundamental grounds. The bridge between a completely phenomenological model, as the 3P_0 model, and more basic ingredients of QCD is far from being established, but the previous works are interesting attempts in that direction.

The 3P_0 model is specially attractive because it can provide the gross features of various transitions with only one parameter, the constant corresponding to the creation vertex. Recently, some of the authors [4] performed a careful study of the improvement obtained for the results coming from the 3P_0 model when more sophisticated forms for the creation vertex are used. When studying strong decays of mesons two uncertainties are present: the creation vertex responsible for the decay and the wave function consequence of the

dynamical treatment of the quark–antiquark interaction. The aim of this paper is to use the improved description of the creation vertex developed in Ref. [4] allied with the wave function for the mesons obtained with the improved dynamical model of Ref. [5].

The paper is organized as follows. In the next section we will analyze the most important features of the dynamical model. Section 3 is devoted to the description of the creation vertex within the 3P_0 method. In Section 4 we will present and discuss the results obtained, comparing with previous parameterizations of the transition vertex and the meson wave functions. Finally, in the last section we will summarize the conclusions of our work.

2. The chiral quark cluster model

Among the different quark models, the chiral quark cluster model is ideally suited to describe the effects of subnucleonic degrees of freedom in few-nucleon systems. The central idea of this model is closely related to the concept of constituent quark mass. Nowadays this mass is viewed as a consequence of the spontaneous chiral symmetry breaking which manifests itself through the appearance of Goldstone fields. Based on these assumptions, Fernández et al. [1] have proposed a potential model where the primary ingredients of the quark–quark interaction are the confining potential and the one-gluon exchange term, for the long- and short-range part of the interaction, respectively. In the intermediate region, between the scale at which the chiral flavor symmetry is spontaneously broken, $\Lambda_{\text{CSB}} \sim 1$ GeV, and the confinement scale, $\Lambda_C \sim 200$ MeV, QCD is formulated in terms of an effective theory of constituent quarks ($m_q \sim M_N/3$) interacting through the Goldstone modes associated with the spontaneous chiral symmetry breaking. The form of this interaction, derived elsewhere [1], includes the following terms:

$$V_{qq}(\vec{r}) = V_{\text{OGE}}(\vec{r}) + V_{\text{CON}}(\vec{r}) + V_{\text{PS}}(\vec{r}) + V_{\text{S}}(\vec{r}), \quad (1)$$

where V_{PS} and V_{S} come from chiral symmetry breaking. The specific form of the central part of these potentials is

$$V_{\text{PS}}(\vec{r}_{ij}) = \frac{1}{3} \alpha_{\text{ch}} \frac{\Lambda_{\text{CSB}}^2}{\Lambda_{\text{CSB}}^2 - m_{\text{PS}}^2} m_{\text{PS}} \left[Y(m_{\text{PS}} r_{ij}) - \frac{\Lambda_{\text{CSB}}^3}{m_{\text{PS}}^3} Y(\Lambda_{\text{CSB}} r_{ij}) \right] \times (\vec{\sigma}_i \cdot \vec{\sigma}_j)(\vec{\tau}_i \cdot \vec{\tau}_j), \quad (2)$$

$$V_{\text{S}}(\vec{r}_{ij}) = -\alpha_{\text{ch}} \frac{4m_n^2}{m_{\text{PS}}^2} \frac{\Lambda_{\text{CSB}}^2}{\Lambda_{\text{CSB}}^2 - m_{\text{S}}^2} m_{\text{S}} \left[Y(m_{\text{S}} r_{ij}) - \frac{\Lambda_{\text{CSB}}}{m_{\text{S}}} Y(\Lambda_{\text{CSB}} r_{ij}) \right], \quad (3)$$

where α_{ch} is the chiral coupling constant and Λ_{CSB} determines the scale at which chiral symmetry is broken. m_n is the mass of the ordinary quark (u or d), m_{PS} the mass of the pseudoscalar Goldstone boson, taken as the experimental π mass, and m_{S} the scalar Goldstone boson mass, which is related to m_{PS} through:

$$m_{\text{S}}^2 = m_{\text{PS}}^2 + (2m_n)^2. \quad (4)$$

The i and j indices are associated with the i th and j th quark, respectively, \vec{r}_{ij} represents the interquark distance, and the $\vec{\sigma}_i$'s ($\vec{\tau}_i$'s) are the spin (isospin) Pauli matrices. $Y(x)$ is the standard Yukawa function defined by

$$Y(x) = \frac{e^{-x}}{x}. \quad (5)$$

The chiral coupling constant α_{ch} is related to the πNN coupling constant $g_{\pi NN}^2$ by

$$\alpha_{\text{ch}} = \left(\frac{3}{5}\right)^2 \frac{g_{\pi NN}^2}{4\pi} \frac{m_\pi^2}{4m_N^2}. \quad (6)$$

As stated above, perturbative effects are included in the model by means of the OGE potential, which is obtained via the nonrelativistic reduction of the one-gluon exchange diagram in QCD [6]. It takes the form:

$$V_{\text{OGE}}(\vec{r}_{ij}) = \frac{1}{4} \alpha_s \vec{\lambda}_i \cdot \vec{\lambda}_j \left\{ \frac{1}{r_{ij}} - \pi \left[\left(\frac{1}{m_i^2} + \frac{1}{m_j^2} \right) + \frac{2}{3m_i m_j} \vec{\sigma}_i \cdot \vec{\sigma}_j \right] \delta(\vec{r}_{ij}) \right\}, \quad (7)$$

where α_s is an effective QCD coupling constant and the $\vec{\lambda}_i$'s are the $SU(3)$ color matrices. When applied to baryons or mesons and in order to avoid an unbound spectrum, the delta function has to be regularized:

$$\delta(\vec{r}) \rightarrow \frac{1}{4\pi} \frac{e^{-r/r_0}}{r_0^2 r}, \quad (8)$$

where r_0 is taken to be $r_0 = 0.094$ fm, a constant value whatever the quarks under consideration.

Finally, we consider the confinement potential that takes into account other QCD nonperturbative effects. Although a lot of evidence exists that the non-abelian nature of QCD leads to confinement of color charge, little is known about it. The main bulk of data comes from lattice QCD simulations. These calculations establish short-range linear rising forces between two static color sources [7,8]. However, pair creation screens the potential at large distances [9]. The screened static potential fitted to results of lattice calculations is given by

$$V_{\text{CON}}(\vec{r}_{ij}) = -a \vec{\lambda}_i \cdot \vec{\lambda}_j (1 - e^{-\mu r_{ij}}). \quad (9)$$

At short distances this potential has a linear type behavior with an effective confinement strength $a_c = a \cdot \mu$.

The parameters of the model are listed in Table 1. Except for the confinement constant, that does not affect the baryon–baryon interaction, all the parameters are taken from the NN sector, see Ref. [10], and translated to the $q\bar{q}$ sector through the G -parity of the corresponding field. This set of parameters guarantees that the binding energy of the deuteron and the NN phase shifts are correctly reproduced. To make a thoughtful comparison with other potential models, the noncentral parts of the interaction, tensor and spin–orbit forces (which are not essential in the meson sector), will not be included in the calculation.

The values for these parameters are in rough agreement with what could be expected from other approaches motivated by QCD. The confining parameter $a_c = 0.2$ GeV fm^{−1} leads to a string tension value $b = 16a_c/3 = 1.06$ GeV fm^{−1}, slightly higher to what is of common use in hadron spectroscopy. This is due to the screening property, as expressed by

Table 1
Quark model parameters for the χ QM potential

$m_{u,d}$ (MeV)	313	
m_s (MeV)	560	
α_s	0.485	
α_{ch}	0.028	
m_S (fm $^{-1}$)	3.42	
m_{PS} (fm $^{-1}$)	0.7	
Λ_{CSB} (fm $^{-1}$)	4.2	
a (MeV)	500.0	} $a_c = 200 \text{ MeV fm}^{-1}$
μ (fm $^{-1}$)	0.4	

Eq. (9). To obtain the same overall quality by integration over the whole range of separation coordinates, one needs a larger slope at the origin to compensate the saturation at large distance.

In Figs. 1 and 2 we present some of the results obtained within this potential model for the meson spectrum. The quality of the results is comparable to any other potential model with the advantage that this calculation is to some extent parameter-free. As previously said, except for confinement, all the other parameters are taken for the two-baryon sector.

In order to test the influence of the wave function, we will compare our results with those obtained with another quark–antiquark potential, the AL1 potential [11–13]. This potential is rather traditional, since it is merely an extension of the usual funnel potential (Coulomb + linear) of the Cornell group or of Bhaduri et al. [14,15]. The main difference lies in the hyperfine term, for which the regularized delta function is chosen of gaussian type and with a size r_0 that is mass dependent. Thus, this potential can be considered as a sophisticated version of the simple Coulomb + linear term. However, all the parameters, that can be found in Ref. [11–13] are obtained by a fit on the experimental mesonic resonances, and in a sense, it is largely more phenomenological than the χ QM presented before.

3. The 3P_0 model

The 3P_0 model is used for many years without fundamental modifications. Basically it corresponds to a quark pair creation from multigluon exchange, with the quantum numbers of the vacuum. We do not want to spend too much time on it, and refer for example to Ref. [17] for complete information. The angular spatial part of the transition operator T is a solid harmonic in a P wave, but the radial amplitude $\gamma(p)$ is a priori anything. Most of calculations performed with this model adopted a constant value, with the argument that it is simple enough and gives acceptable results. Recently, however, it was shown that a momentum dependent term is preferable [4]. The exact form of $\gamma(p)$ is not very important if it has a good shape in the relevant p -range values. In particular the “constant + Gaussian” form is specially attractive because it leads to analytical and simpler expressions. Thus, in our calculations we will also use this form:

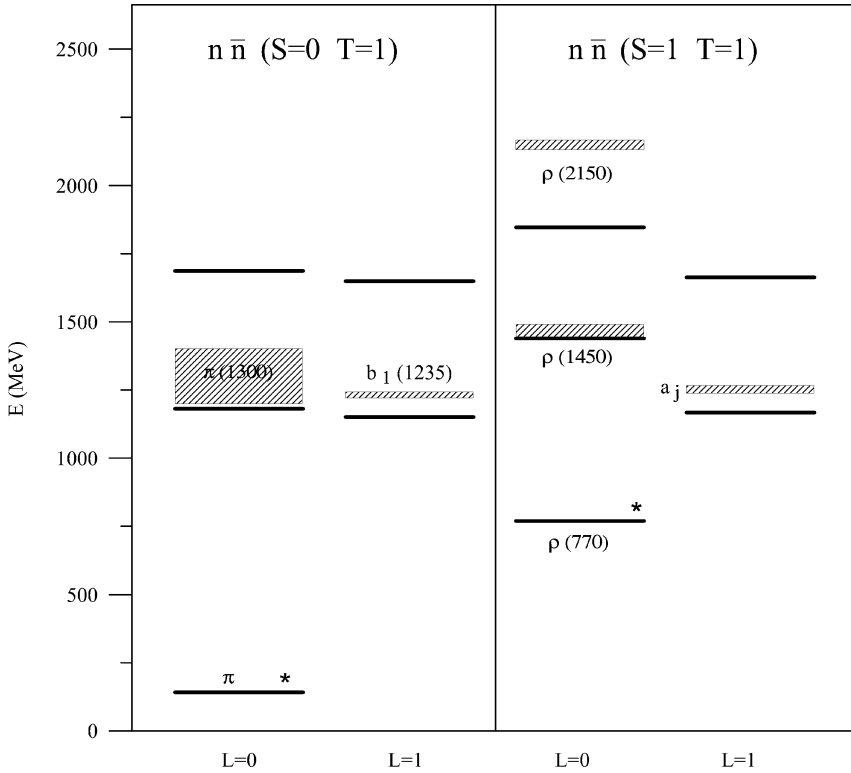


Fig. 1. Comparison of experimental (shadow boxes and thin solid lines quoted with the name of the state appearing in the *Particle Data Book*) and calculated (solid lines) spectra of isovector mesons. Experimental data are taken from Ref. [16]. n stands for u or d quarks. The lines labeled with a “ \star ” represent states where the calculated and the experimental data cannot be distinguished. The experimental data for the 3P_J states correspond to the centroid of the multiplet.

$$\gamma(p) = \gamma_1 + \gamma_2 \exp(-\gamma_3 p^2). \tag{10}$$

We will use a different parametrization for ordinary quark pair creation ($\gamma_n(p)$) and for strange quark pair creation ($\gamma_s(p)$).

We are interested in the partial width $\Gamma_{A \rightarrow BC}$ corresponding to the decay of meson A into mesons B and C . We can adopt a coupling based on angular momentum so that, denoting J_{bc} the total spin of (BC) and l the relative angular momentum between B and C , one has:

$$\Gamma_{A \rightarrow BC} = \sum_{J_{bc}, l} \Gamma_{A \rightarrow BC}(J_{bc}, l), \tag{11}$$

where the partial width corresponding to quantum numbers J_{bc}, l is related to the transition amplitude M through the golden rule:

$$\Gamma_{A \rightarrow BC}(J_{bc}, l) = 2\pi \int dk \delta(E_i - E_f) |M_{A \rightarrow BC}(k)|^2. \tag{12}$$

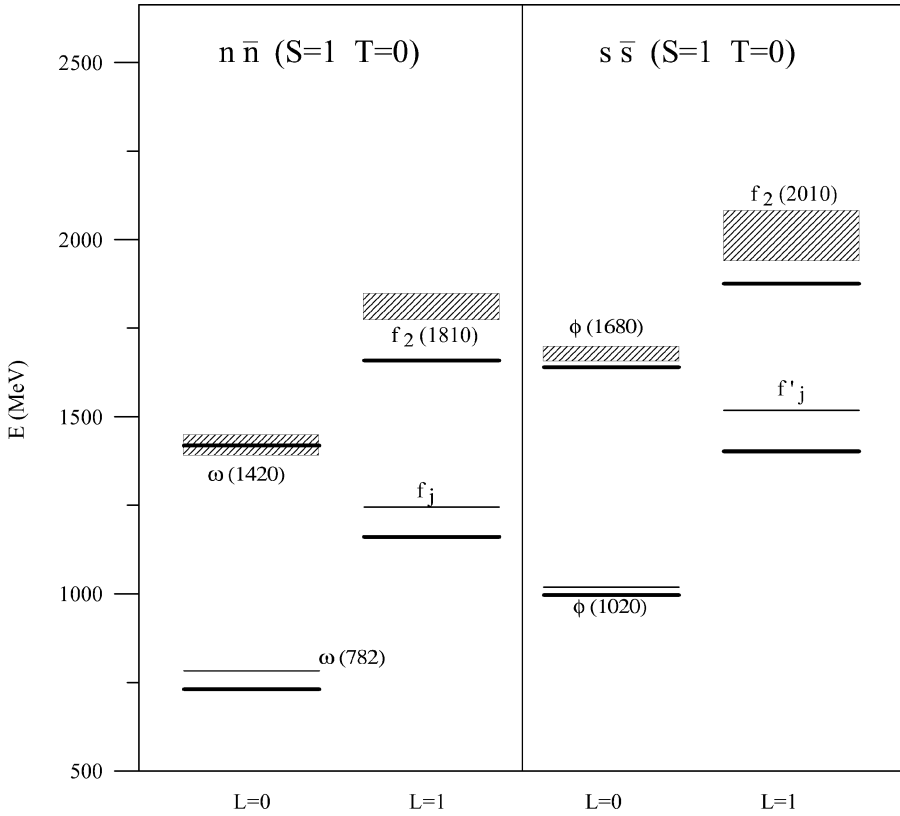


Fig. 2. Same as Fig. 1, but for isoscalar mesons.

The result for this integral on k , the relative momentum of B and C mesons, depends on which phase space is retained. Since our wave functions are essentially obtained from a nonrelativistic method, it would be tempting to use a nonrelativistic phase space. However the phase space factor is mainly a kinematical quantity, which should be disconnected to the dynamical treatment of the wave functions. In Ref. [4] both a relativistic and a nonrelativistic phase space factors have been investigated carefully and the conclusion was that a relativistic phase space must be employed in any case. In this paper we follow this prescription and write:

$$\Gamma_{A \rightarrow BC}(J_{bc}, l) = 2\pi \frac{E_b(\tilde{k}) E_c(\tilde{k})}{m_a \tilde{k}} |M_{A \rightarrow BC}(\tilde{k})|^2, \tag{13}$$

$$\tilde{k} = \frac{\sqrt{[m_a^2 - (m_b - m_c)^2][m_a^2 - (m_b + m_c)^2]}}{2m_a}, \tag{14}$$

with $E_b(\tilde{k}) = \sqrt{m_b^2 + \tilde{k}^2}$ and $E_c(\tilde{k}) = \sqrt{m_c^2 + \tilde{k}^2}$.

The transition amplitude $M_{A \rightarrow BC}(\tilde{k})$ is calculated by successive decoupling and recoupling manipulations, isolating the various degrees of freedom. The result takes the form:

$$M_{A \rightarrow BC}(k) = \frac{1}{\sqrt{1 + \delta_{BC}}} \mathcal{I}(A \rightarrow BC) \sum_{L_{bc}, L, S} \mathcal{C}(A \rightarrow BC) \mathcal{E}(A \rightarrow BC, k), \quad (15)$$

where $\mathcal{I}(A \rightarrow BC)$ is a term depending only on isospin, $\mathcal{C}(A \rightarrow BC)$ is a term coupling spin and space angular momenta and $\mathcal{E}(A \rightarrow BC, k)$ is a pure space term. L_{bc}, L, S are intermediate spin quantum numbers coming from the decoupling procedure. The space term $\mathcal{E}(A \rightarrow BC, k)$ is, by far, the most complicated and the most time consuming factor. Nevertheless, if the meson wave functions are expanded on gaussian amplitudes, the space term can be calculated exactly and analytically. We refer the reader to Ref. [4] for the various expressions and for deeper discussion.

Let us mention two things. First, the 3P_0 operator is not galilean invariant so that the resulting space factor does depend on the chosen reference frame. As usual, we calculate it in the frame where meson A is at rest. For mysterious reasons, it appears that this is a good choice. Indeed, the effect of changing the rest frame was never seriously undertaken and represents a very hard task, much far from the aim of this paper. Second, since there is no tensor force present at the level of the quark–antiquark potential, orbital angular momentum L_a and spin S_a for any meson A are good quantum numbers and the coupling term $\mathcal{C}(A \rightarrow BC)$ and the space term $\mathcal{E}(A \rightarrow BC, k)$ are simplified, at least numerically.

Let us also mention that in the calculation of the basic amplitude $M(A \rightarrow BC)$ four different diagrams contribute: two of them correspond to OZI forbidden diagrams and they are discarded completely (for a discussion of the origin of the OZI rule in connection with fundamental QCD, see, i.e., [18]) and, among the other two, only one contributes in general by a suitable labeling of the mesons B and C in the final channel.

4. Results and discussion

We apply the previous formalism to the known experimental decays of a meson into two mesons. We always work with a relativistic phase space. In the evaluation of the phase space factor, the experimental masses are employed; this is very important in order to get reasonable results. We also work with exact meson wave functions. To be sure of this point, we expand the wave function, obtained by solving the Schrödinger equation with the Numerov algorithm, on a combination of gaussian functions (this is a necessary step to apply our formalism without approximation). We checked, both numerically and graphically, that the “exact” and the “approximate” wave functions are identical over the whole range of variables. It was discussed in Ref. [4] that an exact versus approximate wave function is not so crucial to obtain reasonable results. The harmonic oscillator approximation, which is used by many people, could have been employed as well to give similar results (we checked the results of Ref. [3] in the case of the HO with 0 quanta and recovered the values given in this paper). However a gaussian expansion is much more suitable for a numerical treatment and needs only very few terms to recover the exact wave function (in contrast to the HO expansion). Generally three to six terms in the expansion are enough to insure a good convergence. As already said, we compare the results obtained with two different sets of wave functions:

- (i) those obtained with AL1 potential which is essentially composed of one gluon exchange and linear confining potentials with a gaussian regularized delta function in the hyperfine term (see [4] or [11–13] for more details); it is of type “Coulomb + linear” in spirit, and the parameters were obtained phenomenologically. The meson and baryon spectra are reasonably reproduced with it, and the hadron–hadron interaction has never been checked.
- (ii) those obtained with the χ QM potential presented in the second section. It is more fundamental in the sense that the most important driving parameters are deduced from basic QCD; it gives good results both for meson and baryon spectrum and for nucleon–nucleon properties.

It is interesting to see the sensitivity of the results with respect to these two different potentials. The corresponding wave functions in momentum space look very often quite different, as is exhibited in Fig. 4 where the π and η wave functions are plotted with both potentials. Other differences will be stressed later on.

In order to test the improvement obtained with a momentum dependent 3P_0 vertex $\gamma(p)$ we perform the calculations with both AL1 and χ QM wave functions, considering a “constant” vertex and a “constant + Gaussian” vertex (see definition (10) and Fig. 3). Let us remind that we allow different vertices for an ordinary quark (n quark) pair creation and for a strange quark (s quark) pair creation. To compare also with previous calculations found in literature, we also report the results obtained with the flux tube model (a variant of the 3P_0 model) studied by Kokoski and Isgur [22] (hereafter denoted KI).

Let us emphasize that KI used an ad hoc phase space that improves a lot the results, but which seems to us completely artificial and hardly justified from a physical point of view. Other studies considering some mesonic resonances as glueballs or hybrids have been reported in the literature (see, i.e., [19,20]), but are not commented in this work.

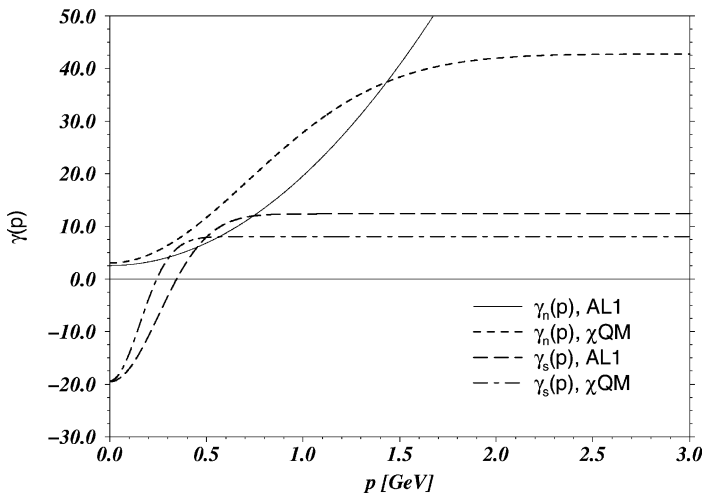


Fig. 3. Momentum dependent vertex $\gamma(p)$ obtained from the wave functions resulting from a Schrödinger equation based on both potentials.

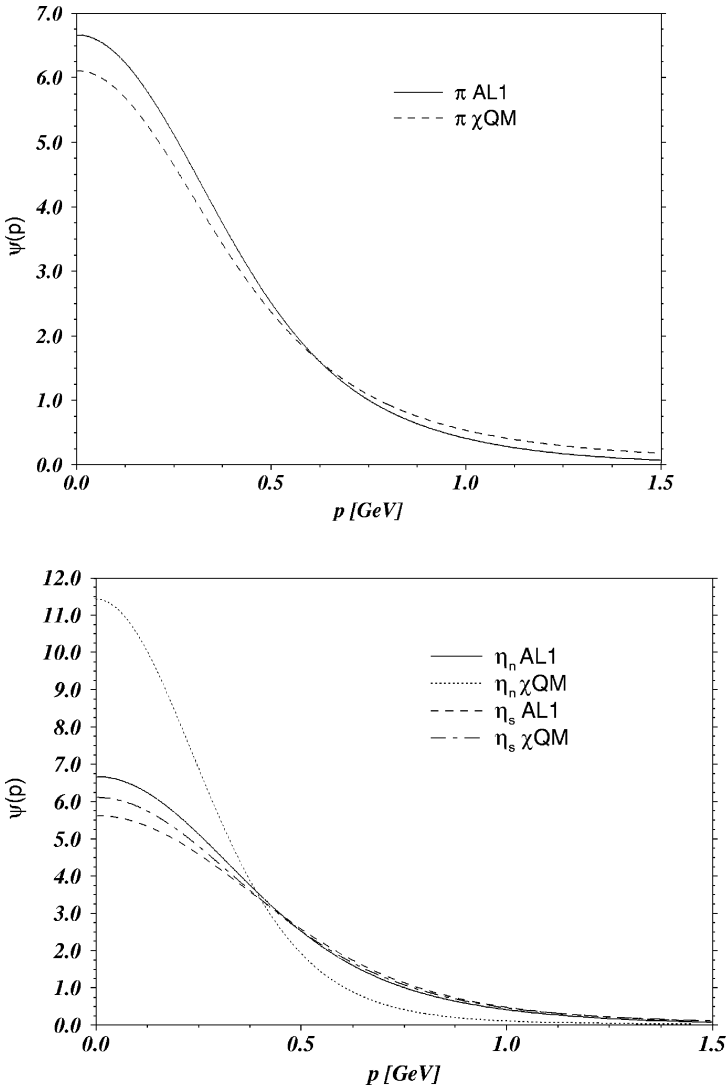


Fig. 4. Comparison of the π and η wave functions in momentum space for the AL1 and χ QM potentials (η_n is the $n\bar{n}$ component and η_s is the $s\bar{s}$ component of the η meson).

To avoid a too large dispersion in our results, we present in our tables the square root of the partial width $\Gamma^{1/2}$ (expressed in $\text{MeV}^{1/2}$). In Tables 2 and 3, we report the transitions well known experimentally and for which each of the decaying meson has a narrow width (less than 50 MeV). The formalism presented in the third section applies without modification.

Several comments are in order. Since the spin-orbit force is absent both in AL1 and χ QM, the $S = 1$ multiplet states (for example $K_0^*(1430)$ and $K_2^*(1430)$) have the same radial wave function. Of course they have different quantum numbers and the coupling

Table 2

Square root of the partial widths $\Gamma^{1/2}$ [MeV^{1/2}] corresponding to decays with final mesons having a narrow width (< 50 MeV). This is the set used for determining the parameters of the dynamical transition vertex. The first eight transitions provide with γ_n and the three last ones with γ_s

Decay	$\gamma = \gamma_1 + \gamma_2 e^{-\gamma_3 p^2}$		$\gamma = \gamma_1$		Flux tube	
	AL1	χ QM	AL1	χ QM	Kok.	Exp.
$\rho \rightarrow \pi\pi$	9.96	9.44	8.60	7.85	12.4	12.28 ± 0.37
$\phi \rightarrow K\bar{K}$	1.97	2.12	1.76	1.97	2.5	1.92 ± 0.06
$K^*(892) \rightarrow \pi K$	5.79	6.12	5.12	5.38	6.5	7.08 ± 0.21
$f_2(1270) \rightarrow \pi\pi$	11.81	10.61	12.85	11.05	8.9	$12.53^{+0.23}_{-0.13}$
$f_2(1270) \rightarrow \eta\eta$	0.45	1.41	0.98	2.11	0.9	0.91 ± 0.10
$f_2'(1525) \rightarrow K\bar{K}$	8.98	11.48	9.13	11.15	6.5	8.06 ± 0.56
$K_2^*(1430) \rightarrow \pi K$	8.74	9.88	8.98	9.45	6.5	7.01 ± 0.21
$K_2^*(1430) \rightarrow \omega K$	1.35	1.94	2.11	2.77	1.4	1.70 ± 0.23
$a_2(1320) \rightarrow K\bar{K}$	2.31	2.29	3.01	3.04	2.8	2.29 ± 0.19
$f_2(1270) \rightarrow K\bar{K}$	2.91	2.96	2.46	2.49	2.7	2.92 ± 0.13
$f_2'(1525) \rightarrow \eta\eta$	2.74	1.94	3.26	2.76	2.5	2.80 ± 0.46

factor $\mathcal{C}(A \rightarrow BC)$ is different even if the final channel is identical. Tensor force is also absent, so that L is a good quantum number and ρ , ω , K^* are pure 3S_1 states, a_2 , f_2 , K_2^* are pure 3P_2 states, etc. Notice that $f_2(1270)$ is a $n\bar{n}$ resonance and $f_2'(1525)$ is a $s\bar{s}$ resonance.

Contrary to AL1, χ QM potential contains an isospin dependent term (see Eq. (2)) so that ρ and ω , or a_2 and f_2 have different radial wave functions. This is a basic difference between both potentials. The η wave function is, as usually postulated, $(n\bar{n} - s\bar{s})/\sqrt{2}$; however, in AL1 the $n\bar{n}$ component η_n is identical to the pion wave function, whereas in χ QM it is different, due to the isospin dependence of the potential (this property is clear from a glance at the two parts of Fig. 4). The η' wave function is the orthogonal combination $(n\bar{n} + s\bar{s})/\sqrt{2}$.

It is very likely that the $K_1(1270)$ and $K_1(1400)$ resonances are a mixing of 1P_1 and 3P_1 states. Since the antisymmetric spin-orbit force is absent in both potentials, a mixing angle has to be postulated. However, a dynamical calculation using a sophisticated potential including antisymmetric spin-orbit interaction provides the value 23° . The value given in Ref. [16] corresponds to the one presented by [21], namely close to 45° . We shall adopt here an average value of 34° , as suggested in [23], which gives a slightly better agreement with the data. An additive contribution is effective for $K_1(1270)$ and a subtractive one for $K_1(1400)$, as has been discussed in detail in Ref. [21].

Lastly let us mention a peculiarity arising in some transitions. The γ_n vertex is determined for transitions including a $n\bar{n}$ creation alone. Of course the absolute sign of γ_n is not relevant. The same is valid for the γ_s vertex, which is determined from transitions including a $s\bar{s}$ creation alone. So, for transitions resulting from a pure flavor creation, we have freedom to choose the vertex with an arbitrary overall phase. But some transitions,

Table 3

Square root of the partial widths $\Gamma^{1/2}$ [MeV^{1/2}] corresponding to decays with final mesons having a narrow width (< 50 MeV) determined with the parameters resulting from Table 2. The values χ^2/N of the chi square per transition are calculated on the total set of transitions corresponding to Tables 2 and 3

Decay	$\gamma = \gamma_1 + \gamma_2 e^{-\gamma_3 p^2}$		$\gamma = \gamma_1$		Flux tube	
	AL1	χ QM	AL1	χ QM	Kok.	Exp.
$a_2(1320) \rightarrow \eta\pi$	4.25	6.65	5.64	7.40	4.1	3.94 ± 0.19
$a_2(1320) \rightarrow \eta'\pi$	1.23	1.01	1.60	1.75	0.8	0.75 ± 0.07
$\rho_3(1690) \rightarrow \pi\pi$	8.41	7.08	9.75	7.55	4.6	6.14 ± 0.26
$\rho_3(1690) \rightarrow K\bar{K}$	1.71	0.71	2.84	3.14	2.3	1.59 ± 0.14
$\rho_3(1690) \rightarrow \omega\pi$	7.08	7.62	10.15	9.86	3.9	5.06 ± 0.96
$f_4(2050) \rightarrow \pi\pi$	8.92	6.84	9.82	6.43	3.4	5.95 ± 0.32
$f_4(2050) \rightarrow K\bar{K}$	0.72	3.78	2.26	2.58	1.5	$1.19^{+0.30}_{-0.16}$
$f_4(2050) \rightarrow \eta\eta$	0.87	5.57	1.89	5.16	0.7	0.66 ± 0.13
$f_4(2050) \rightarrow \omega\omega$	7.90	8.22	8.67	8.88		7.35 ± 0.88
$K_1(1270) \rightarrow \omega K$	3.65	4.20	4.16	4.73	4.0	3.15 ± 0.45
$K_1(1400) \rightarrow \omega K$	3.35	3.80	3.57	4.04	1.9	1.32 ± 0.66
$K^*(1410) \rightarrow \pi K$	0.41	1.07	1.06	0.01		3.91 ± 0.42
$K_2^*(1430) \rightarrow \eta K$	1.36	2.94	0.33	1.21	0.7	$0.38^{+0.44}_{-0.13}$
$K_0^*(1430) \rightarrow \pi K$	17.89	15.39	5.77	4.85		16.34 ± 1.24
$K^*(1680) \rightarrow \pi K$	9.01	6.61	3.50	2.08	7.1	11.16 ± 1.94
$K_3^*(1780) \rightarrow \pi K$	7.24	8.27	8.24	8.25	4.0	5.47 ± 0.39
$K_3^*(1780) \rightarrow \eta K$	1.35	2.84	0.15	2.07	2.9	6.91 ± 1.56
$K_4^*(2045) \rightarrow \pi K$	5.24	6.13	6.47	5.99	2.2	4.43 ± 0.29
χ^2/N	18.90	87.66	47.48	100.30	28.94	

for example $K_2^*(1430) \rightarrow \eta K$ or $K_3^*(1780) \rightarrow \eta K$, need both $n\bar{n}$ and $s\bar{s}$ creation vertices to obtain the transition amplitude (this is due to the flavor mixing in the η) and here the relative sign between γ_n and γ_s is very important. In Table 3 we use the sign which gives the better agreement with the data. With the convention of a positive sign at the origin ($\gamma(p=0) > 0$) the relative sign is positive for the constant vertex and negative for the momentum dependent vertex (this corresponds to a positive contribution based on the vertex functions appearing in Fig. 3).

The parameters appearing in the vertex $\gamma(p)$ are fitted for each potential on the eight first transitions of Table 2 for the ordinary quark pair creation, and on the three following ones for the strange quark pair creation. All the other transitions represented in Table 3 are pure predictions for our models. The corresponding vertex functions are presented on Fig. 3.

There exist some differences between both types of $\gamma(p)$ functions. But, more important, one clearly sees that one needs to take different expressions for a n quark pair creation and a s quark pair creation. In particular, the saturation to the constant part of the function is reached for much lower p values for a $s\bar{s}$ creation than for a $n\bar{n}$ creation.

The first interesting impression that we have looking at Tables 2 and 3 is the very big improvement induced by allowing a momentum dependent vertex; this is true for both AL1 and χ QM (let us note that the same conclusion can be drawn from KI although the model is slightly different, but it also corresponds to a momentum dependent vertex). This result, which is transparent just by a glance at the χ^2/N values (χ^2 divided by the number of considered transitions), confirms the tendency observed in Ref. [4] and thus should be considered as more or less universal improvement. The effect goes in the right direction, enhancing or decreasing the values.

Just by looking at the χ^2/N values, the difference between AL1 and χ QM wave functions may seem very big. In fact, the rather bad value for the chi-square in the case of χ QM has its unique origin in a bad description of the η wave function (see also Fig. 4 to see the big difference). As a probe, we recalculated the χ^2/N values, but removing all transitions appearing in Table 3 that include a η in the final channel. The case with a momentum dependent vertex gives 33.79 instead of 87.66 and the case with the constant vertex gives 48.19 instead of 100.30. On the contrary, this change does not affect the AL1 results showing that the trouble is specific to the χ QM potential. This problem culminates in the $f_4(2050) \rightarrow \eta\eta$ transition, in which two η appear in the final state. Moreover, the f_4 is a F-wave meson, which probes outer part of the wave function (in position space) which differs in both potentials.

In general, we have not seen regularities which favor one potential over the other, so that we prefer to say that both give an overall good description of the transitions. The KI model is also good despite the fact that the fit has been done on one decay only ($\rho \rightarrow \pi\pi$). The quality of KI is essentially due to the modified phase space factor. Indeed, we verified, in some specific transitions, that our results are also improved using this ad hoc phase space. But we do not want to introduce it because of lack of justification. The relativistic phase space that we adopted seem to us the only one justified on physical grounds. In view of this remark, we estimate that our results give much better agreement with the physical situation.

In Table 4, we report the results of the known transitions for which one of the final mesons, let say B , is itself unstable and decays predominantly into two mesons B_1 and B_2 with an appreciable width (larger than 50 MeV). The formulae given in the previous section are in principle deficient because, due to the uncertainty on the mass m_b , the \tilde{k} value is no longer fixed but must be varied over a range. In this range, both the transition amplitude and the width vary. The formulae should be modified. We adopted the prescriptions suggested in Ref. [24], which write:

$$\Gamma_{A \rightarrow BC}(J_{bc}, l) = \int_0^{k_{\max}} dk \frac{|M_{A \rightarrow BC}(k)|^2 \Gamma_b(k)}{[M_a - E_b(k) - E_c(k)]^2 + \Gamma_b^2(k)/4}, \quad \text{where} \quad (16)$$

Table 4

Square root of the decay width $\Gamma^{1/2}$ [MeV^{1/2}] with a broad meson in the final channel, obtained with the parameters of the Table 2. The χ^2/N values concern only the transitions appearing in this table. For more details, see text

Decay	$\gamma = \gamma_1 + \gamma_2 e^{-\gamma_3 p^2}$		$\gamma = \gamma_1$		Flux tube	
	AL1	χ QM	AL1	χ QM	Kok.	Exp.
$a_2(1320) \rightarrow \rho\pi$	8.98	9.84	11.51	11.76	7.9	8.66 ± 0.26
$\pi_2(1670) \rightarrow \rho\pi$	13.37	13.47	14.33	14.07	9.5	8.94 ± 0.66
$\pi_2(1670) \rightarrow K\bar{K}^*$	7.61	7.42	3.73	3.02	4.2	2.33 ± 0.56
$\pi_2(1670) \rightarrow f_2(1270)\pi$	11.49	10.94	9.33	9.12	9.2	12.04 ± 0.54
$K_1(1270) \rightarrow \rho K$	8.05	8.96	7.84	8.80	10.0	6.15 ± 0.81
$K_1(1270) \rightarrow \pi K^*(892)$	2.52	2.90	3.62	3.96	2.9	3.80 ± 0.73
$K_1(1270) \rightarrow \pi K_0^*(1430)$	0.36	0.38	0.20	0.19	1.3	5.02 ± 0.66
$K_1(1400) \rightarrow \pi K^*(892)$	14.47	13.86	10.74	10.10	21.0	12.79 ± 0.63
$K_1(1400) \rightarrow \rho K$	6.01	6.94	6.54	7.58	4.0	2.28 ± 1.15
$K_2^*(1430) \rightarrow \pi K^*(892)$	4.74	5.20	6.13	6.28	4.1	4.98 ± 0.16
$K_2^*(1430) \rightarrow \rho K$	3.81	5.10	4.91	6.15	3.4	2.95 ± 0.14
$K^*(1680) \rightarrow \rho K$	4.71	4.54	3.64	3.31	3.9	$10.06^{+1.88}_{-1.76}$
$K^*(1680) \rightarrow \pi K^*(892)$	5.38	5.08	3.70	3.27	4.5	$9.81^{+1.71}_{-1.85}$
$K_3^*(1780) \rightarrow \rho K$	5.49	7.57	7.33	9.03	3.4	7.02 ± 1.12
$K_3^*(1780) \rightarrow \pi K^*(892)$	5.80	5.98	7.83	7.46	3.3	5.64 ± 0.80
$K_4^*(2045) \rightarrow K^*(892)\phi$	9.06	9.30	2.41	1.98		1.66 ± 0.43
χ^2/N	35.34	50.43	36.43	60.11	23.73	

$$k_{\max} = \frac{\sqrt{[m_a^2 - (m_{b_1} + m_{b_2} + m_c)^2][m_a^2 - (m_{b_1} + m_{b_2} - m_c)^2]}}{2m_a}. \quad (17)$$

These prescriptions are essentially empirical, since we do not have any serious criterion to extend correctly the formulae valid for mesons with narrow widths. The dynamical width $\Gamma_b(k)$ should in principle be calculated in the 3P_0 model for the decay $B \rightarrow B_1 B_2$, but in the frame where the momentum of the B meson is k . Due to non-galilean invariance of the transition vertex this obviously leads to problems. Moreover, most of the time, there exist several channels for the decay and formula (16) should itself be modified. So, there is not a unique way to understand this formula. After the use of several “plausible” prescriptions, we chose a compromise by adopting $\Gamma_b(k) = \Gamma_b(\text{exp})$.

From Table 4, we see now that the calculations give much poorer results in this case; in particular a constant vertex seems as well acceptable as a more sophisticated one. The hierarchy in the important transitions is more or less reproduced but the deviations from the experimental values are more pronounced. Here again there is no significative difference between AL1 and χ QM. On the contrary KI gives more acceptable values. The

only explanation for this must be attributed to their rather ad-hoc phase space.

To our opinion the fault of this relatively poor description is not a consequence of bad wave functions but rather of a failure of the modified width formula (16) or/and to the non-galilean invariance of the 3P_0 model.

The partial width $\Gamma_{A \rightarrow BC}$ is very sensitive to the phase space factor, which is essentially a kinematical quantity. To concentrate more on the dynamics and to get rid of the phase space effect, it has been argued [3] that a good observable is the ratio $M(A \rightarrow (BC)_D)/M(A \rightarrow (BC)_S)$ when two partial waves D and S are present in the final state. Some values are known experimentally. The same can be done with F/P or G/D ratios, sometimes with different values of J_{bc} . There exists a lot of transitions presenting such a D/S , F/P or G/D mixing. In Table 5 only the most interesting ones are presented; when a broad meson is present in the final channel it is considered as stable (otherwise it remains uncertainties that result from Eq. (16) which gives directly a width and not an amplitude).

In this study, the values coming from a constant vertex look again very different from those coming from a momentum dependent vertex. One can often find a difference by a factor two to four and, for the $\pi_2 \rightarrow KK^*$, the sign itself is different. The values arising from a momentum dependent vertex are in closer agreement with experimental data, when they are known. This confirms once more the superiority of a momentum dependent vertex.

The values derived from both kinds of wave functions (AL1 and χ QM) always have the same sign and are of the same order of magnitude, the deviation being more sensitive for higher partial waves. Let us note that in one case ($\pi_2 \rightarrow KK^*$) the partial wave with high relative angular momentum ($l = 3$) is dominant over the wave with low angular momentum ($l = 1$). So, the tendency observed for the partial widths is confirmed totally at the inner level of partial wave mixing. As quoted in Ref. [3] we verified that the ratio of the D/S amplitude ratios ($a_1 \rightarrow \rho\pi/b_1 \rightarrow \omega\pi$) is rather independent of the model with a value close to the one ($-1/2$) given by a harmonic oscillator approximation.

5. Summary

In this paper, we investigate whether the description of strong transitions is sensitive to the details of the meson wave functions. We compare two different sets of wave functions resulting from two different quark–antiquark interactions. Both contain confining terms, and one-gluon exchanges, but the χ QM contains in addition effects coming from Goldstone boson exchanges. The resulting wave functions may be sometimes very different. Nevertheless the results concerning the decay of a meson into two mesons seems to be of comparable quality, if we forget the case of η resonance which raises problems with χ QM.

On the other hand, we showed that using a momentum dependent vertex at the level of the 3P_0 transition operator improves significantly the agreement with the experimental data. This is certainly the most important dynamical ingredient to be retained in the 3P_0 model, since the improvement is clear whatever the wave functions used in the calculations. In any case, it allows a drastic improvement in the results. There exists probably a deep

Table 5

Selected ratios for the amplitudes between partial widths resulting from both potentials (AL1 and χ QM) and for both types of transition vertex (Gauss. refers to the momentum dependent vertex $\gamma(p) = \gamma_1 + \gamma_2 \exp(-\gamma_3 p^2)$ and Cte to the constant vertex $\gamma = \gamma_1$). The experimental values, when known, are indicated in parenthesis under the transitions. A number of transitions (i.e., $\pi_2 \rightarrow f_2\pi$) contain a mixing $l = 0, 2, 4$ and thus appear both in the D/S part and G/D part

Partial wave	Decay	AL1		χ QM	
		Gauss.	Cte	Gauss.	Cte
D/S	$b_1 \rightarrow \omega\pi$ (+0.29 ± 0.04)	+0.332	+0.624	+0.363	+0.686
	$a_1 \rightarrow \rho\pi$ (−0.100 ± 0.028)	−0.181	−0.353	−0.215	−0.399
	$h_1 \rightarrow \rho\pi$	+0.247	+0.458	+0.295	+0.539
	$\pi_2 \rightarrow f_2\pi$	+0.298	+0.470	+0.369	+0.595
	$K_2(1770) \rightarrow \pi K_2^*(1430)$	+0.245	+0.355	+0.273	+0.401
	$K_2(1770) \rightarrow f_2K$	+0.007	+0.009	+0.008	+0.010
	$K_2(1820) \rightarrow \pi K_2^*(1430)$	+0.120	+0.153	+0.133	+0.174
F/P	$K_2(1820) \rightarrow \omega K$	−0.683	−1.618	−1.013	−2.510
	$\pi_2 \rightarrow \rho\pi$	+0.973	+2.610	+1.398	+3.960
	$\pi_2 \rightarrow KK^*$	−2.069	+0.369	−2.220	+0.465
	$K_2(1770) \rightarrow \pi K^*$	+0.952	+2.210	+1.201	+2.849
G/D	$\pi_2 \rightarrow f_2\pi$	+0.074	+0.084	+0.089	+0.107
	$K_2(1770) \rightarrow \pi K_2^*(1430)$	+0.067	+0.086	+0.077	+0.100
	$K_2(1770) \rightarrow f_2K$	+0.002	+0.002	+0.002	+0.002
	$K_2(1820) \rightarrow \pi K_2^*(1430)$	−0.169	−0.256	−0.198	−0.293
	$K_3^*(1780) \rightarrow \pi K_2^*(1430)$	+0.063	+0.075	+0.068	+0.082
	$\omega_3(1670) \rightarrow b_1\pi$	+0.081	+0.106	+0.112	+0.141
$\frac{G(J_{bc}=0)}{D(J_{bc}=2)}$	$f_4 \rightarrow \omega\omega$	−0.231	−0.554	−0.876	−0.351
$\frac{G(J_{bc}=2)}{D(J_{bc}=2)}$	$f_4 \rightarrow \omega\omega$	+0.457	+1.097	+1.736	+0.696
$\frac{G(J_{bc}=0)}{D(J_{bc}=2)}$	$K_4^*(2045) \rightarrow K^*(892)\phi$	−0.139	−0.044	−0.174	−0.050
$\frac{G(J_{bc}=2)}{D(J_{bc}=2)}$	$K_4^*(2045) \rightarrow K^*(892)\phi$	+0.276	+0.087	+0.345	+0.100

relationship between this momentum dependence and basic QCD, but we do not see how to prove it. This would be very difficult and the answer is hidden in the nonperturbative behavior of QCD.

The calculations are also sensitive to the wave functions since χ QM and AL1 can give relatively different answers. But it appears that none of them is superior for the whole set of data; for reasons not yet understood the final quality is of the same degree. Since, in a sense, the chiral model is “more fundamental” (or less phenomenological!) we are happy to see that it can lead to very good results as well. This conclusion is valid not only at the level of the partial widths but also at the level of the mixing of various partial waves inside the same transition.

When a meson with large width is present in the final state, the results are deteriorated appreciably. The fault is obviously due to the weakness of the used formula (but we did not find alternative ones in literature), or to the non-galilean invariance of the model. We think that a correct theoretical description in the framework of the 3P_0 model is not available for the moment in this case.

Acknowledgements

L.A.B. thanks the Ministerio de Educación y Ciencia for financial support. This work has been partially funded by Dirección General de Investigación Científica y Técnica (DGICYT) under the Contract No. PB97-1410 and by a IN2P3-CICYT agreement.

References

- [1] F. Fernández, A. Valcarce, U. Straub, A. Faessler, J. Phys. G 19 (1993) 2013.
- [2] P. Geiger, E.S. Swanson, Phys. Rev. D 50 (1994) 6855.
- [3] E.S. Ackleh, T. Barnes, E.S. Swanson, Phys. Rev. D 54 (1996) 6811.
- [4] R. Bonnaz, B. Silvestre-Brac, Few-Body Syst. 27 (1999) 163.
- [5] L.A. Blanco, F. Fernández, A. Valcarce, Phys. Rev. C 59 (1999) 438.
- [6] A. de Rújula, H. Georgi, S.L. Glashow, Phys. Rev. D 12 (1975) 147.
- [7] G.S. Bali, K. Schilling, A. Wachter, Phys. Rev. D 56 (1997) 2566.
- [8] G.S. Bali, Fizika 38 (1999) 229.
- [9] K.D. Born et al., Phys. Rev. D 40 (1989) 1653.
- [10] A. Valcarce, A. Buchmann, F. Fernández, A. Faessler, Phys. Rev. C 50 (1995) 2240.
- [11] B. Silvestre-Brac, C. Semay, ISN 93-69, unpublished.
- [12] B. Silvestre-Brac, Few-Body Syst. 20 (1996) 1.
- [13] C. Semay, B. Silvestre-Brac, Z. Phys. C 61 (1994) 271.
- [14] E. Eichten, K. Gottfried, T. Kinoshita, J. Kogut, K.D. Lane, T.M. Yan, Phys. Rev. Lett. 34 (1975) 369.
- [15] R.K. Bhaduri, L.E. Cohler, Y. Nogami, Nuovo Cimento A 65 (1981) 376.
- [16] Particle Data Group, Eur. Phys. J. C 3 (1998) 1.
- [17] A. Le Yaouanc et al., Hadron Transitions in The Quark Model, Gordon and Breach, New York, 1988.
- [18] P. Geiger, N. Isgur, Phys. Rev. Lett. 67 (1991) 1066; Phys. Rev. D 44 (1991) 799; Phys. Rev. D 47 (1993) 5050.

- [19] F.E. Close, P.R. Page, Nucl. Phys. B 443 (1995) 233.
- [20] T. Barnes, F.E. Close, P.R. Page, E.S. Swanson, Phys. Rev. D 55 (1997) 4157.
- [21] H.G. Blundell, S. Godfrey, B. Phelps, Phys. Rev. D 53 (1996) 3712.
- [22] R. Kokoski, N. Isgur, Phys. Rev. D 35 (1987) 907.
- [23] W. Roberts, B. Silvestre-Brac, Phys. Rev. D 57 (1998) 1964.
- [24] S. Capstick, W. Roberts, Phys. Rev. D 49 (1994) 4570.